Nonlinear Dynamical Aspects of Atomic Scale Friction

W.G. Conley, A. Raman and C.M. Krousgrill

Purdue University School of Mechanical Engineering
585 Purdue Mall, West Lafayette, IN, 47907, USA, raman@ecn.purdue.edu

ABSTRACT

This work presents a detailed computational and analytical investigation of Tomlinson's model for atomic scale dry friction. The model describes a prototypical mechanism of energy dissipation from an atom dragged across a periodic atomic lattice and is often used to model the dynamics of friction force microscope tips and for the atomistic sliding of adsorbate layers on surfaces. While a number of articles in the literature utilize this model, there is little work in the literature that utilizes the computational and theoretical tools of modern nonlinear dynamics in analyzing this model.

This research demonstrates that the use of computational nonlinear dynamics techniques provides a deep insight into the mechanisms of chaotic stick-slip phenomena and the speed dependence of frictional forces of atomic scale friction.

Keywords: Friction, Nonlinear, Dynamics, Atomic-Scale, Nanoscale

1 INTRODUCTION

It is estimated that a lack of understanding of friction accounts for a $420 billion waste every year in the US alone [1]. The accurate modeling and control of dry friction is important in a number of technological applications including space robots and satellites, hard disk drives, automobile disk brakes, MEMS devices, nanoscale lithography, imaging and data storage. Investigations of the fundamental mechanisms of friction at the atomic scale can (i) help design electromechanical devices at the micro and nano scale and (ii) help understand how the modification of surfaces at the nanoscale can modify the frictional properties at the macroscale.

Atomic scale friction is usually studied using discrete models of atoms or particles dragged across atomic lattices. Several works model phonon dynamics at such interfaces [1]; however the fundamental resonance interactions underpinning these processes are difficult to extract from these models. In this regard Tomlinson's model is a simple single degree of freedom nonlinear model of a single atom oscillator or an elastic asperity dragged at a constant speed over a rigid, periodic lattice. Some numerical simulations of Tomlinson's model [2]–[5] have been confirmed by friction force microscopy [6]–[8]. The resonance dynamics of Tomlinson's model were investigated by Helman *et al.* [9]. This study investigated a combination of dry and lubricated friction which demonstrated the existence of chaotic responses and a variety of bifurcations located at integer and fractional multiples of the resonance frequencies of the oscillator.

The present work extends the work of Helman *et al.* to include a comprehensive investigation of the fundamental instability mechanisms in the model. Further modern computation techniques such as AUTO are used to explore the boundaries between stable and unstable solutions. This analysis cannot be achieved through traditional methods. This work also explains the origin of large frictional forces arising when the excitation frequency is approximately twice the natural frequency of the oscillator. Finally, key implications of the velocity dependence of friction force are discussed.

2 MODEL

A sketch of Tomlinson's model is shown in Figure 1. The model is also used to model lateral vibrations of friction force microcantilever (FFM). From the model, we can derive the equation of motion for this one dimensional system. In the model the potential term, $V = -V_0 \cos(\frac{2\pi x}{a} + \frac{2\pi v}{a} t)$, produces a nonlinear coupling between the response and time as shown in Equation (1).

$$\frac{d^2y}{d\tau^2} + 2\zeta\frac{dy}{d\tau} + y = A\sin(y + \Omega\tau) \qquad (1)$$

Note that in Equation (1), the y coordinate system is referenced to the inertial sliding support. Subsequent analysis is performed for $\zeta = 0.1$, while A and Ω are varied. A is directly proportional to the depth of the potential well while Ω is directly proportional to the speed of translation and inversely proportional to the lattice spacing.

3 SLOW DYNAMICS

For $\Omega << 1$ only one stable periodic orbit was found. A typical example of this type of motion is shown if Figure 2. This motion resembles stick-slip motion observed at the macroscale. The tip remains in a potential well

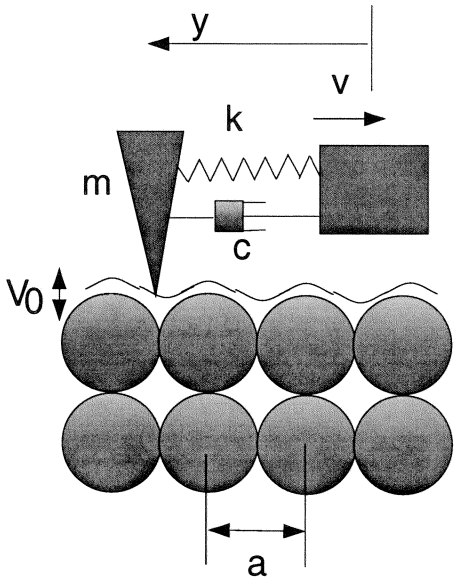

Figure 1: Sketch of a typical FFM model

until the stretching spring snaps the tip out of the well. This snapout is characterized by high frequency transients which rapidly decay. This process repeats itself periodically.

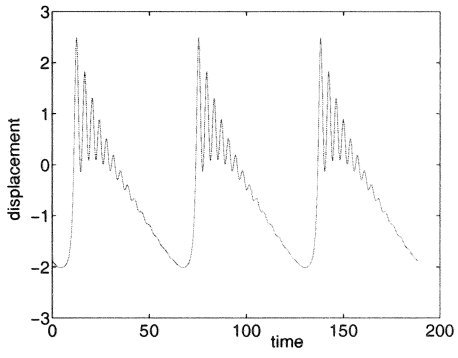

Figure 2: Displacement Response for $A = 2$, $\Omega = 0.1$

When $\Omega << 1$, the transients have sufficient time to damp out before encountering the next snap through phenomenon. This fast-slow dynamic is typical at slow speeds.

4 RESONANCE DYNAMICS

As the speed increases further, the resonance dynamics near $\Omega = 2, 1, \frac{1}{2}, \frac{1}{3}, ...$ are very complex. A variety of tools are used to analyze these regions.

AUTO is a powerful tool for analyzing nonlinear differential equations employing a continuation algorithm [10]. AUTO requires a stable orbit either at a frequency either above or below the resonance frequency; AUTO then continues that orbit into the resonance regions. A typical plot of AUTO's response is provided for $A = 2$, as seen in Figure 3. In this figure the bold lines are the stable solutions while the thin lines are unstable solutions. From this figure we see that regions of instabilities are nearly centered at integer and fractional multiples of the natural frequency.

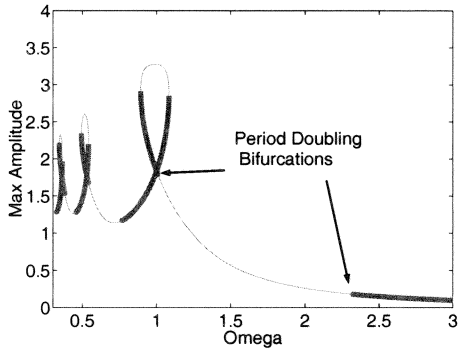

Figure 3: AUTO Computed amplitude response for A=2

While the large amplitude responses near $\Omega = 1/3$, $1/2$ and 1 are due to superharmonic and primary resonances, the study of the instability near $\Omega = 2$ is facilitated through a linearization of Equation (1). For small vibration amplitudes, the linearization of (1) leads to

$$\ddot{y} + y(1 + A\cos(\Omega\tau) = A\sin(\Omega\tau) \qquad (2)$$

Equation (2) is the Mathieu's equation with external forcing. A variety of analytical techniques exist for determining the stability boundaries for the homogeneous solutions in Mathieu's equation. Stability boundaries are generated using AUTO computations and using perturbation techniques with A as the perturbation parameter. The perturbation method is based on Jordan and Smith [11]. The AUTO results and analytically estimated stability boundaries are shown in Figure 4.

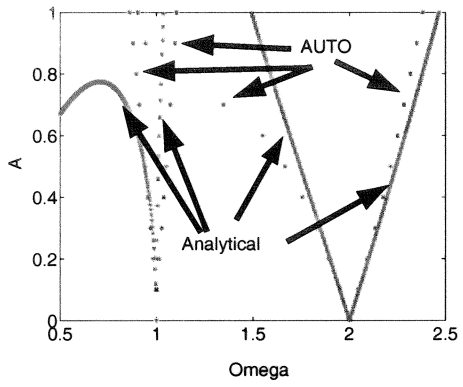

Figure 4: Stability Boundaries

The results correlate well for small values of A. As A increases the assumptions of no damping and small oscillations combined with the asymptotic expansion technique causes the discrepancies between the two different techniques. The agreement for small A supports the theory that resonance behavior around $\Omega = 2$ is due to a parametric instability in Equation (1).

To examine the regions of parametric instability, an analysis of the bifurcations in the system was performed using continuation methods. By providing a stable orbit for either a small or large Ω, the evolution of the solution is tracked as Ω changes. A bifurcation diagram for $A = 1.5$ is shown in Figure 5.

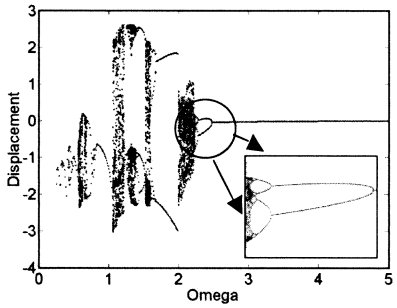

Figure 5: Bifurcation Diagram for $A = 1.5$

The period doubling cascade which occurs around the parametric instability is located near the values predicted by AUTO. Again, the parametric excitation plays a key role in the analysis.

To fully examine the behavior in this region Poincaré maps are created. An example is shown at $\Omega = 2$ and $A = 5.9$. Since these parameters are located in an unstable region, complex behavior is expect; Figure 6 shows that chaotic behavior occurs for these parameters.

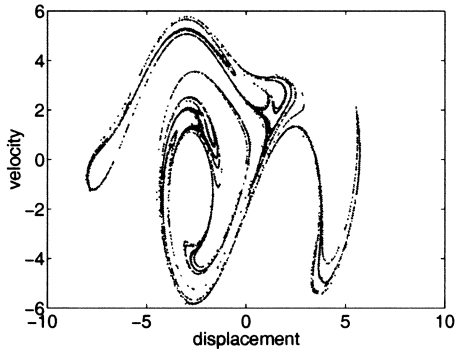

Figure 6: Poincaré map for $A = 5.9$ and $\Omega = 2$

A variety of different initial conditions result in similar Poincaré maps. These maps show that the sliding response is stable, but not periodic.

5 HIGH SPEED DYNAMICS

For $\Omega >> 1$, multiple stable solutions may exist. For a small initial condition, the magnitude of the response will stay small and converge to a period 1 solution. A large initial condition however, may stay large and converge to a higher period solution. An example of this motion occurs at $A = 2$ and $\Omega = 5$. The Poincaré map for both initial conditions is shown in Figure 7. A small initial condition is shown with the large dots, which approach a stable period 1 solution while the large initial condition results in a stable period 5 solution, shown by the small dots.

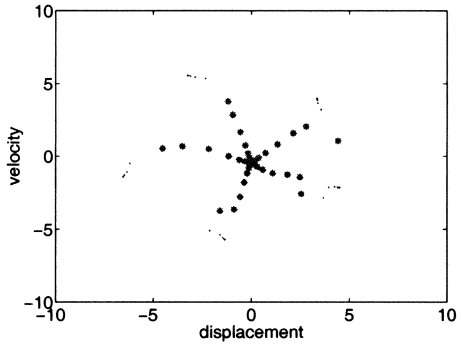

Figure 7: Poincaré Map for Large Ω

These dynamics are unique to the choice of $A = 2$ and $\Omega = 5$. A perturbation away from $\Omega = 5$ causes all solutions to tested initial conditions to converge to a period 1 solution. A perturbation away from $A = 2$ maintains the two unique stable solutions.

6 FRICTIONAL FORCE

In the regions where the dynamics become complex due to bifurcations and chaotic motion it is useful to analyze the system using a root mean square (RMS) value. The RMS of the force required to move the base of the cantilever at a constant velocity is plotted in Figure 8. The plot is generated from the force time histories with each time history being averaged over 10,000 atoms. To provide some scaling to this figure, typically the natural frequency of a FFM tip is on the order of 100 kHz. On a silicon sample, the primary resonance would occur at a support velocity near 10 μm/s.

A interesting feature on this plot is the resonance behavior. The peak around the primary resonance, $\Omega = 1$, is indicative of a forced response. While the abrupt transition to the peak around $\Omega = 2$ correlates to a parametric instability. The location of the instability correlates perfectly with the results of Figure 4. Again, this supports the theory that parametric instabilities are the cause of this peak.

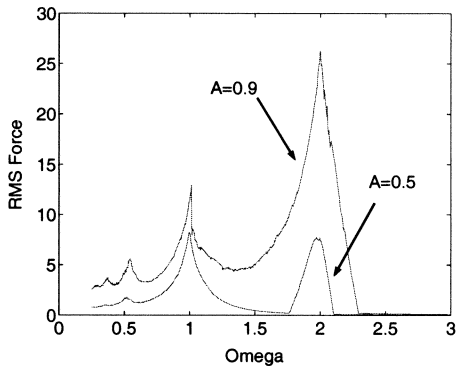

Figure 8: RMS of the friction force

A similar analysis can be performed on the superharmonics. These peaks are also due to the parametric instabilities in the system. An interesting question which is raised concerns the period doublings which occur between the superharmonics since no noticeable change occurs in the response at these values. Further investigation is required to understand the behavior in these regions.

A final consideration from Figure 8 is the force required to initiate motion of the cantilever base. Due to finite computing resources, it is not possible to analyze the $\lim \Omega \rightarrow 0$. However, an analytical solution is quite simple for this case. As Ω becomes small, $\ddot{y}$ and $\dot{y}$ will become small for all but a very brief instant in time. Equation (1) can be reduced to

$$y = A \sin(y + \Omega\tau)$$

This equation demonstrates that the maximum possible displacement is $y = A$. An analysis of the relationship between the normal force and A is required before determining that a static coefficient of friction is related linearly to the normal force. While $y = A$ is the maximum value, the RMS value as $\Omega \rightarrow 0$ will be less than A.

7 CONCLUSIONS

This paper has shown that chaotic behavior is present in Tomlinson's model. A cascade of period doubling occurs in the transition from predictable behavior to chaos. Modern nonlinear mechanics tools, such as AUTO, enable the study of these complex dynamics. Analytical techniques have confirmed the numerical simulations. From this result and the RMS responses for a variety of different A values, we have determined that parametric excitation plays an important role in exciting this system, the larger A becomes the more important the parametric term becomes.

In the transition between stick slip oscillations and steady sliding, a variety of rich dynamics are observed. A greater understanding of these rich dynamics will allow for more accurate control of materials sliding at low velocities. At high speed, Tomlinson's model predicts a very small frictional force. A revision in the model may be required to more accurately describe sliding friction. Additionly, experimental verification of the rich dynamics is required.

REFERENCES

[1] B.N.J. Persson, "Sliding Friction: Physical Principles and Applications 2nd Edition," Springer, 2000.

[2] M.Porto, V. Zaloj, M. Urakh and J. Klafter, "Macroscopic versus microscopic description of friction: from Tomlinson model to shearons," Tribology Letters, 9, 45-54, 2000.

[3] V.Zaloj, M. Urbkh and J. Klafter, "Deducing energy disipation from rheological response," Journal of Chemical Physics, 110, 1263-1266, 1999.

[4] T. Baumberger and C. Caroli. "A phenomenology of boundary lubrication: the lumped junction model," Euopean Physical Journal B, 4, 13-23, 1998.

[5] B.N.J. Persson, "Theory of friction: The role of elasticity in boundary lubrication," Physical Review B, 50, 4771-4786, 1994.

[6] O. Zwörner, H. Hölscher, U.D. Schwarz and R. Wiesendanger, "The velocity dependence of frictional forces in point-contact friction," Applied Physics A, 66, S263-S267, 1998.

[7] O.K. Dudko, A.E. Filppov, J. Klafter, M. Urbakh, "Dynamic force spectroscopy: a Fokker=Planck approach," Chemical Physics Letters, 352, 499-504, 2002.

[8] E. Gnecco, R. Bennewitz, T.Gyalog, Ch. Loppacher, M. Bammerline, E. Meyer and H.-J. Güntherodt, "Velocity Dependence of Atomic Friction," Physical Review Letters, 84, 1172-1175, 2000.

[9] J.S. Helman, W. Baltensperger and J.A. Holyst, "Simple model for dry friction," Physical Review B, 49, 3831-3838, 1994.

[10] E.J. Doedel, A.R. Champneys, T.F. Fairgrieve, Y.A. Kuznetsov, B .Sandstede and X. Wang, "AUTO 97: Continuation and Bifurcation software for Ordinary Differential Equations (with HomCont)," http://www.cs.concoria.ca/auto, 1998.

[11] D.W. Jordan and P. Smith, "Nonlinear Ordinary Differntial Equations 3rd Edition," Oxford, 1999.